

Adsorption on carbon nanotubes: quantum spin tubes, magnetization plateaus, and conformal symmetry

Dmitry Green^a and Claudio Chamon^b

^a *Department of Physics, Yale University, New Haven, CT 06520*

^b *Department of Physics, Boston University, Boston, MA 02215*

We formulate the problem of adsorption onto the surface of a carbon nanotube as a lattice gas on a triangular lattice wrapped around a cylinder. This model is equivalent to an XXZ Heisenberg quantum spin tube. The geometric frustration due to wrapping leads generically to four magnetization plateaus, in contrast to the two on a flat graphite sheet. We obtain analytical and numerical results for the magnetizations and transition fields for armchair, zig-zag and chiral nanotubes. The zig-zags are exceptional in that one of the plateaus has extensive zero temperature entropy in the classical limit. Quantum effects lift up the degeneracy, leaving gapless excitations which are described by a $c = 1$ conformal field theory with compactification radius quantized by the tube circumference.

PACS: 67.70+n, 71.10.Pm, 75.10.Jm,

Monolayer adsorption of noble gases onto graphite sheets has proven to be an interesting problem both theoretically and experimentally [1–3]. Many of the observed features can be understood within a lattice gas model, where the underlying hexagonal substrate layer forms a triangular lattice of preferred adsorption sites. An equivalent formulation is in the language of spin models on a triangular lattice, where the repulsion between adsorbed atoms in neighboring sites translates into an antiferromagnetic Ising coupling. The frustration of the couplings by the triangular lattice leads to the rich phase diagram of the monolayer adsorption problem [2]. Introducing hopping adds quantum fluctuations, further enriching the phase diagram [3,4].

In this paper we address what happens if, in addition to the triangular lattice frustration, one has an extra geometric frustration due to periodic boundary conditions. In fact, such a system is physically realized by a single walled carbon nanotube [5], which may be viewed as a rolled graphite sheet. In this context, adsorption has been the subject of growing experimental and theoretical interest [6,7] spurred by potential applications. Stan and Cole [6] have considered the limit of non-interacting adatoms at low density, finding that they are localized radially near a nanotube’s surface at a distance comparable to that in flat graphite ($\sim 3\text{\AA}$). In that work, it was sufficient to omit the hexagonal structure of the substrate. However, the corrugation potential selects the hexagon centers as additional commensurate localization points [1]. In view of the similarity to flat graphite, we include both the substrate lattice and adatom interactions and consider a wider range of densities. In fact, very recently, it has been shown [8] that the adsorbate stays within a cylindrical shell for fillings less than $\approx 0.1/\text{\AA}^2$ (or ≈ 0.5 adatom/hexagon), justifying the densities studied here.

The adsorption sites thus form a triangular lattice wrapped around a cylinder. The geometrically inequivalent ways in which the wrapping is realized are labeled

by two integers, (N, M) ; the case (N, N) is known as the armchair tube, $(N, 0)$ is the zig-zag, and all others are chiral. The geometric frustration is present whenever the wrapping destroys the tripartite nature of the triangular lattice, which occurs when $(N - M) \bmod 3$ is non-zero (this criterion is familiar in the context of electronic conductivity [5]). Thus, both zig-zag and chiral tubes can be frustrated geometrically, whereas armchair tubes cannot. In Fig. 1 we show the tube obtained from the $(7, 0)$ zig-zag. In terms of the equivalent spin systems, this is similar to recent models of “spin tubes” [9].

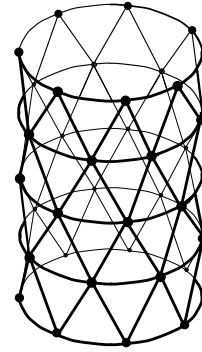


FIG. 1. Adsorption sites on a $(7, 0)$ zig-zag nanotube

When the adsorbed gas is a hard-core boson, the lattice gas is defined by the Bose-Hubbard Hamiltonian [3,10]

$$\mathcal{H} = -t \sum_{\langle ij \rangle} b_i^\dagger b_j + b_j^\dagger b_i + V \sum_{\langle ij \rangle} n_i n_j - \mu \sum_i n_i, \quad (1)$$

where n_i is the boson density at site i , V is the nearest neighbor repulsion and t is the hopping amplitude. In the equivalent Heisenberg spin representation,

$$\mathcal{H} = -2t \sum_{\langle ij \rangle} S_i^x S_j^x + S_i^y S_j^y + V \sum_{\langle ij \rangle} S_i^z S_j^z - H \sum_i S_i^z, \quad (2)$$

where $S_i^z = n_i - 1/2$ and $H = \mu - 3V$ is an effective

external magnetic field. Throughout the paper we will use the spin and density representations interchangeably.

The Ising limit, in which hopping is not allowed, already contains many interesting features. We start the analysis in this regime, obtaining the phase diagram as a function of the magnetic field, and then consider quantum fluctuations perturbatively in t/V . We summarize our results first.

The phase diagram in the temperature-magnetic field plane of a typical tube is shown in Fig. 2.

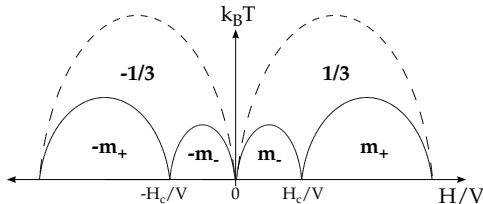


FIG. 2. Phase diagram of the (N, M) tube

When the index $q = (N - M) \bmod 3$ is 1 or 2, we find four lobes (solid lines), corresponding to two plateaus with magnetizations $m_- < 1/3$ and $m_+ > 1/3$. Here, we use the standard Ising notation in which spin is ± 1 . Note that the plateaus are real phases only at zero temperature because the tube is one-dimensional. At finite temperature, the boundaries should be interpreted as crossovers. Nonetheless, deep within a lobe, at $k_B T \ll V$, the magnetizations are well-defined. Specifically, for $q = 1$, we obtain the exact expressions

$$m_+ = \frac{1}{3} \left(1 + \frac{2}{2M + N} \right) \quad m_- = \frac{1}{3} \left(1 - \frac{2}{2N + M} \right)$$

$$H_c = \left(4 - \frac{2M}{N + M} \right) V \quad (3)$$

The complementary case of $q = 2$ is obtained by interchanging $N \leftrightarrow M$. On the other hand, those tubes without geometric frustration ($q = 0$) behave similarly to the flat sheet (dotted lines) which has only two lobes with magnetizations $\pm 1/3$ [2]. As the tube perimeter approaches the flat sheet limit, one expects that the geometric frustration becomes irrelevant. Indeed, as N or $M \rightarrow \infty$, m_+ and m_- squeeze $1/3$ as the inverse of the tube diameter and become indistinguishable. Beyond the lobes, where the field is strong enough to overcome all nearest neighbor bonds ($|H|/V > 6$ at $k_B T = 0$), the tube is fully polarized. The filling fractions are obtained from the magnetizations by $m = -2(n - 1/2)$. The phase diagram, however, is more easily visualized in terms of spin since spin reversal, $m \leftrightarrow -m$, corresponds to particle-hole symmetry, $n \leftrightarrow 1 - n$.

We have verified this prediction numerically by transfer matrix methods for zig-zag tubes up to $N = 11$ and for the chiral tubes up to $N + M = 7$. Although 7 is probably too small to be physical, we believe that the arguments

in this paper generalize to any tube. In Fig. 3 we display sample data for two zig-zag tubes with different q : $(7, 0)$ and $(8, 0)$. The magnetization curves show clear plateaus whose values and transition fields match those predicted by Eq. (3). By increasing the temperature and following the evolution of the plateaus, we generate the phase diagram above.

We find that a rather interesting feature of the zig-zag $(N, 0)$ tubes emerges, making them exceptional. The insets in Fig. 3 indicate an extensive entropy at zero temperature, which has plateaus, too. Upon enumerating the degenerate space explicitly, we shall show that the entropy is exactly $s = (\ln 2)/N$ and that it occurs in m_+ for $q = 1$ and in m_- for $q = 2$. In the presence of hopping, the non-degenerate plateaus retain their gaps, whereas the degenerate ones become correlated states with a unique ground state and *gapless* excitations. More precisely, conformal invariance develops and the effective theory has central charge $c = 1$ with a compactification radius, R , quantized by the tube circumference, $R = N$.

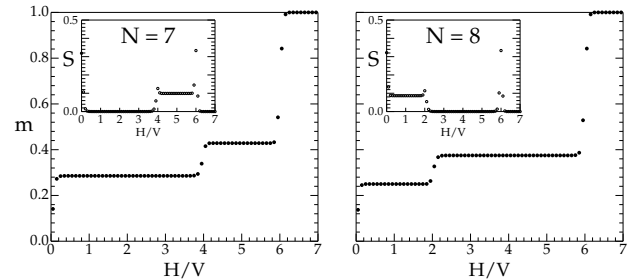


FIG. 3. Magnetization and entropy per site at $k_B T = 0.05V$

In order to understand the magnetizations and nature of the geometric frustration, it is more intuitive to use the original bosonic picture. As a result of hard-core repulsion on the infinite graphite sheet, the $m = 1/3$ plateau corresponds to filling one of the three sublattices, A, B or C , of the triangular lattice. This configuration minimizes the repulsion, $V n_i n_j$, while maximizing the filling, μn . It is natural to try the same for nanotubes, as we illustrate in Fig. 4 for $(5, 0)$.

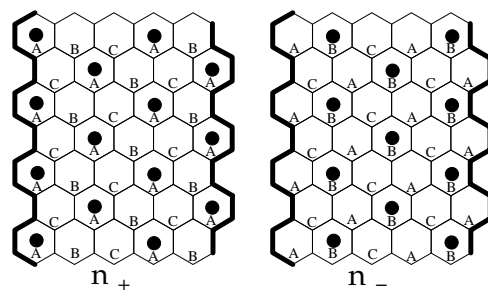


FIG. 4. Fillings and zipper of the $(5, 0)$ zig-zag tube. n_{\pm} corresponds to m_{\mp}

Upon wrapping, however, the thick vertical lines are identified and the lattice is no longer tripartite. In fact, the number of sublattice sites is no longer equal, and there is a mismatch along the thick line, which we term the “zipper”. On the left we fill the A sublattice, obtaining the filling fraction $n_+ = 2/5$, and on the right either B or C may be filled with the result that $n_- = 3/10$. For general $(N, 0)$ there are $2N$ hexagons in the unit cell, and the filling fractions are $n_+ = \lceil 2N/3 \rceil / 2N$ and $n_- = \lfloor 2N/3 \rfloor / 2N$, where $\lceil x \rceil$ and $\lfloor x \rfloor$ denote the larger and smaller of the two bounding integers of x , respectively. The magnetizations in Eq. (3) follow directly by using the correspondence $m = -2(n - 1/2)$. Furthermore, due to the sublattice mismatch, the number density of adjacent particles, n_b , may be non-zero. In the case of $(5, 0)$, there are two broken bonds per unit cell in n_+ , and none in n_- . This result generalizes to any $q = 2$ zig-zag tube: $n_{b+} = 2/2N$ and $n_{b-} = 0$. For $q = 1$, the argument goes through as before, except that $n_{b+} = 1/2N$. We summarize this compactly by $n_{b+} = q/2N$.

Substituting these fillings into the Hamiltonian (1) yields two energies per site, $e_{\pm}(\mu) = Vn_{b\pm} - \mu n_{\pm}$. The transition occurs when these levels cross: $e_+ = e_-$, or

$$\frac{q}{2N} - \mu \frac{\lceil 2N/3 \rceil}{2N} = -\mu \frac{\lfloor 2N/3 \rfloor}{2N} \quad (4)$$

Solving for μ and using the correspondence $H = \mu - 3V$ gives precisely the critical field in Eq. (3). In particular, this explains why there are exactly two independent plateaus. Note that, for the special case of the zig-zags, the critical field depends only on q and not on N per se.

In the above analysis, we have made only one assumption, namely that the zipper runs parallel to the tube axis. In general, the zipper may wind helically around the tube or wiggle sideways. However, in all the cases that we considered, the straight zipper has the lowest energy, and moreover, our transfer matrix computations, which are blind to this assumption, are consistent with our analysis.

The chiral tubes are different. Due to their geometry the zipper is forced to wind, but, again, we find that the choice of the straightest possible zipper reproduces our numerics for $N + M$ up to 7. The determination of the fillings and level crossings is much more involved than that of the zig-zag, and we leave it for a more detailed paper. In any case, our analysis reveals that the plateaus in a chiral tube are not macroscopically degenerate, so that the zig-zags are at a special degenerate point.

Having understood in detail the Ising limit, we now turn on a small hopping, $t \ll V$, that introduces quantum fluctuations. Deep within a plateau, the substrate is maximally filled since adding a particle increases n_b . Consequently, all plateaus begin with a classical gap of order V , and we work in the Hilbert space of the classical ground states. Those plateaus which have only a discrete

symmetry must retain their gaps, but the macroscopically degenerate plateaus are more complicated.

Let us reconsider the n_+ filling of the $(5, 0)$ tube in Fig. 4. Notice that a particle may hop laterally by one site without changing n_b , as we illustrate in Fig. 5, left. Imagine building a typical n_+ state layer-by-layer from top to bottom, with a total of L layers. Each new layer must add exactly two filled sites and one nearest-neighbor bond ($n_b = 1/5$). This constraint implies that no two adjacent sites may be occupied within a layer; if they were, then, to conserve n_b , two adjacent sites must be occupied in the next, and so on up the tube. However, this state is not connected to any other by a single hop. Similarly, the particles cannot hop from layer to layer because this adds another intra-layer bond.

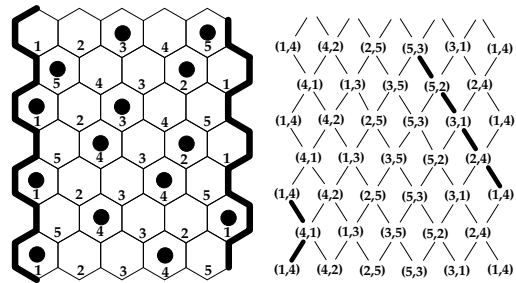


FIG. 5. LEFT: Typical configuration in n_+ (or m_-) of the $(5, 0)$ tube. Alternating numbering within layers allows a symmetric description from bottom-to-top or top-to-bottom. RIGHT: Allowed states as paths on a wrapped square lattice. The vertex labels may be dropped.

An allowed state can be represented as a string of occupied sites, $\{\sigma_i\}$, $i = 1, \dots, L$, which in our example is $\{\dots(5, 3)(5, 2)(3, 1)(2, 4)(1, 4)(1, 4)\dots\}$. At each layer, there are exactly two possibilities for the following one. For example, $(1, 4)$ can be followed by $(1, 4)$ or by $(2, 4)$. However, the total number of possibilities at any given level is five. Fig. 5 (right) summarizes this structure succinctly as a *square* lattice wrapped on the cylinder. A typical state, then, is a lattice path along the tube.

Generalizing to $(N, 0)$, we find N possible states in each layer and two in the succeeding one, and the structure of states is again that of a wrapped square lattice with N squares along the circumference. The dimension of the Hilbert space is the number of lattice paths, $N2^L$, so that in an infinitely long tube, the entropy per site is exactly $(\ln 2)/N$, as claimed earlier. Notice that constrained paths introduce correlations along the length of the tube, despite the absence of inter-layer hopping.

The matrix elements of the projected Hamiltonian connect only those states that differ by a single hop:

$$\langle \{\tau\} | \mathcal{H} | \{\sigma\} \rangle = \begin{cases} -2t & \text{if } \sum_i \delta_{\sigma_i \tau_i} = L - 1 \\ 0 & \text{otherwise} \end{cases} \quad (5)$$

We diagonalize this Hamiltonian numerically with periodic boundary conditions for system sizes up to $N = 11$

and $L = 10$. Additionally, we can obtain the ground state energy up to $L = 16$ due to the sparseness of \mathcal{H} . We will fix $2t = 1$ in what follows.

We find that the degeneracy is lifted and the ground state becomes unique and uniform. The ground state energy, $E_0(L)$, follows $E_0 \sim -0.607L - \pi c/6$ with $c \sim 1.005$. The lowest $N - 1$ excited states are given by $\Delta_a = a^2 \Delta / (N^2 L)$, with $\Delta = 12.9 \pm 0.5$, which is shown in Fig. 6 for $a = 1, 2, 3$. All of these levels are doubly degenerate.

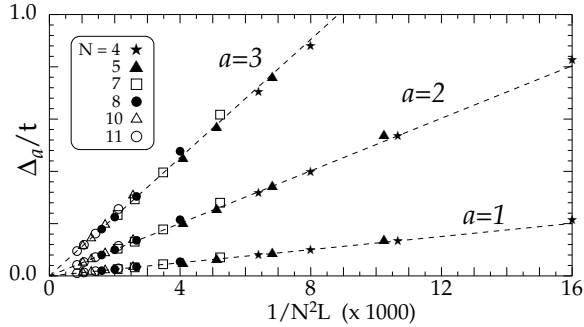


FIG. 6. The gap scales as $1/N^2 L$.

This ground state energy and spectrum are in perfect agreement with a conformally invariant bosonic theory with central charge $c = 1$ compactified on a radius $R = \zeta N$. We take the Lagrangian density $\mathcal{L} = \frac{1}{8\pi} [v^{-1}(\partial_t \phi)^2 - v(\partial_x \phi)^2]$, where v is a velocity, and the compactification is defined by $\phi \equiv \phi + 2\pi R$. The zero mode energies of this theory are [11]

$$E_{a,b}^0 = \frac{2\pi v}{L} \left(\frac{a^2}{R^2} + \frac{b^2 R^2}{4} \right), \quad (6)$$

where a, b are integers that label topological momenta and windings of ϕ . Right- and left-moving oscillator modes of energy $\omega_n = v k_n$, where $k_n = 2\pi n/L$, also appear in the spectrum, but for $a < N$ the zero modes are the lowest. Our spectrum in Fig. 6 corresponds to $E_{a,b}^0$ with $b = 0$. To fix ζ , we look at higher low-lying levels (which also scale like $1/L$). We find that the N 'th excitation energy is independent of N and quadruply degenerate. This can happen only if the N 'th zero mode, $E_{\pm N,0}^0 = 2\pi v/\zeta^2 L$, is degenerate with the lowest oscillator mode, $\omega_{\pm 1} = 2\pi v/L$, which fixes $\zeta = 1$. Thus, the compactification radius is $R = N$. The velocity can be read off from the slopes in Fig. 6 as $v = \Delta/2\pi$. The rest of our spectrum is consistent with these parameters.

One observable consequence of conformal symmetry is that the low temperature heat capacity is fixed by c [11]:

$$C = c \frac{\pi k_B^2}{3} T = \frac{\pi k_B^2}{3} T \quad (7)$$

It is noteworthy that, even though the dispersion of the oscillator modes is independent of N , the spectrum remembers, via the zero-modes, the finite radius of the

nanotube. Furthermore, R is quantized by N ; in the language of Luttinger liquids, this means that the Luttinger parameter is fixed by topology, similarly to the case of edge states in a fractional quantum Hall fluid [12], and in contrast to quantum wires (where the Luttinger parameter can vary continuously). Because there is no inter-layer hopping, ϕ is tied to transverse, rather than to longitudinal, density fluctuations along the tube. We will present a detailed analytical derivation of the effective theory from the lattice in Fig. 5 elsewhere.

Let us briefly view the spin tube as a quantum spin ladder to see if it yields the zero gap. A standard approach is to use a Lieb-Schultz-Mattis (LSM) argument, in which the spins are deformed slowly along the length [13]. Applying it to our tube, we find that a plateau is gapless if $S - M$ is not an integer, where S is the total spin and M the magnetization per layer. Using $S = N/2$ and the magnetizations from Eqn. (3), we find that $S - M$ is an integer in the macroscopically degenerate plateaus, so that the LSM argument is insufficient in this case. A conclusive argument must take the geometric frustration into account.

Before concluding, we should point out that the geometry of the $(2, 0)$ tube is special; all sites in adjacent layers are interconnected. As a result, all of its plateaus have an extensive entropy, and we find that hopping opens a gap in both plateaus. In fact, this tube can be written as a spin chain that has been studied at isotropic coupling [14], $-2t = V$. Two plateaus were found in this case, and it is tempting to speculate whether the two regimes are connected adiabatically.

In conclusion, we have studied the problem of monolayer adsorption on carbon nanotubes and identified several interesting filling fraction plateaus. Since the difference between the plateaus decreases slowly, as the inverse of the tube diameter, experimental measurement should be feasible for large enough tubes. We have identified the zig-zag tubes as exceptional, in which the geometric frustration together with quantum fluctuations lead to conformal symmetry. This system is a physical realization of quantum spin tubes.

The authors wish to thank C. Buragohain, M. El-Batanouny, E. Fradkin, N. Read, C. Nayak, M. Vojta, and X.-G. Wen for helpful comments. Support was provided by the NSF Grant DMR-98-18259(D. G.), DMR-98-76208 and the Alfred P. Sloan Foundation (C. C.).

-
- [1] M. Bretz, J. Phys. Col. **39**, C6/1348-51 (1978).
 - [2] M. Schick, J. S. Walker and M. Wortis, Phys. Rev. B **16**, 2205 (1977).
 - [3] G. Murthy, D. Arovas, A. Auerbach, Phys. Rev. B **55**, 3104 (1997).
 - [4] R. Moessner, S. L. Sondhi and P. Chandra, cond-mat/9910499.
 - [5] *Science of Fullerenes and Carbon Nanotubes*, M. S. Dress-

- selhaus, G. Dresselhaus and P. C. Eklund, Academic Press (1996).
- [6] G. Stan and M. W. Cole, Surf. Sci. **395**, 280 (1998).
 - [7] G. Stan, M. J. Bojan, S. Curtarolo, S. M. Gatica, M. W. Cole, cond-mat/0001334.
 - [8] S. M. Garcia, G. Stan, M. M. Calbi, J. K. Johnson and M. W. Cole, cond-mat/0004229.
 - [9] E. Orignac, R. Citro and N. Andrei, cond-mat/9912200.
 - [10] *Interacting Electrons and Quantum Magnetism*, A. Auerbach, Springer-Verlag (1994).
 - [11] P. Ginsparg in *Fields, Strings and Critical Phenomena*, E. Brezin and J. Zinn-Justin, eds., Elsevier (1988); J. L. Cardy, *ibid*.
 - [12] X. G. Wen, Phys. Rev. B **41**, 12838 (1990).
 - [13] M. Oshikawa, M. Yamanaka and I. Affleck, Phys. Rev. Lett. **78**, 1984 (1997).
 - [14] T. Sakai and N. Okazaki, cond-mat/0002113.